

University of Dundee

Gene deletions leading to a reduction in the number of cyclopentane rings in *Sulfolobus acidocaldarius* tetraether lipids

Guan, Ziqiang; Delago, Antonia; Nußbaum, Phillip; Meyer, Benjamin H; Albers, Sonja-Verena; Eichler, Jerry

Published in:
FEMS Microbiology Letters

DOI:
[10.1093/femsle/fnx250](https://doi.org/10.1093/femsle/fnx250)

Publication date:
2018

Document Version
Peer reviewed version

[Link to publication in Discovery Research Portal](#)

Citation for published version (APA):

Guan, Z., Delago, A., Nußbaum, P., Meyer, B. H., Albers, S-V., & Eichler, J. (2018). Gene deletions leading to a reduction in the number of cyclopentane rings in *Sulfolobus acidocaldarius* tetraether lipids. *FEMS Microbiology Letters*, 365(1), 1-8. [fnx250]. <https://doi.org/10.1093/femsle/fnx250>

General rights

Copyright and moral rights for the publications made accessible in Discovery Research Portal are retained by the authors and/or other copyright owners and it is a condition of accessing publications that users recognise and abide by the legal requirements associated with these rights.

- Users may download and print one copy of any publication from Discovery Research Portal for the purpose of private study or research.
- You may not further distribute the material or use it for any profit-making activity or commercial gain.
- You may freely distribute the URL identifying the publication in the public portal.

Take down policy

If you believe that this document breaches copyright please contact us providing details, and we will remove access to the work immediately and investigate your claim.

20 **ABSTRACT**

21 The cell membrane of (hyper)thermophilic archaea, including the thermoacidophile
22 *Sulfolobus acidocaldarius*, incorporate dibiphytanylglycerol tetraether lipids. The
23 hydrophobic cores of such tetraether lipids can include up to eight cyclopentane rings.
24 Presently, nothing is known of the biosynthesis of these rings. In the present study, a
25 series of *S. acidocaldarius* mutants deleted of genes currently annotated as encoding
26 proteins involved in sugar/polysaccharide processing were generated and their glycolipids
27 were considered. Whereas the glycerol-dialkyl-glycerol tetraether core of a *S.*
28 *acidocaldarius* tetraether glycolipid considered here mostly includes four cyclopentane
29 rings, in cells where the *Saci_0421* or *Saci_1201* genes had been deleted, species
30 containing zero, two or four cyclopentane rings were observed. At the same time, in cells
31 lacking *Saci_0201*, *Saci_0275*, *Saci_1101*, *Saci_1249* or *Saci_1706*, lipids containing
32 mostly four cyclopentane rings were detected. Although *Saci_0421* and *Saci_1201* are
33 not found in proximity to other genes putatively involved in lipid biosynthesis,
34 homologues of these sequences exist in other Archaea where cyclopentane-containing
35 tetraether lipids are found. Thus, *Saci_0421* and *Saci_1201* represent the first proteins
36 described that somehow contribute to the appearance of cyclopentane rings in the core
37 moiety of the *S. acidocaldarius* glycolipid considered here.

38 **INTRODUCTION**

39 The lipids that comprise biological membranes serve to distinguish Archaea from
40 Eukarya and Bacteria. In eukaryal and bacterial membranes, phospholipids essentially
41 comprise fatty acid side chains linked to a 1,2-sn-glycerol-3-phosphate backbone via
42 ester bonds. In contrast, archaeal phospholipids contain isoprenoid hydrocarbon side
43 chains linked to a 2,3-sn-glycerol-1-phosphate backbone via ether bonds (Koga and Morii
44 2007; Villanueva et al. 2014). While many Archaea organize such lipids, mainly based on
45 a diphytanylglycerol diether (archaeol) hydrophobic core yet presenting different head
46 groups, into a bilayer structure, (hyper)thermophilic archaea contain membranes that are
47 based on varying ratios of such lipids and dibiphytanylglycerol tetraether lipids. In
48 dibiphytanylglycerol tetraether lipids, two 40 carbon-long isoprenoid chains are ether-
49 linked to glycerol backbones at each end or to a glycerol or a calditol group at either end,
50 which in turn, can present different head groups (Chong 2010; Chong et al. 2012). These
51 hydrophobic cores of tetraether lipids, i.e., caldarchaeol (or glycerol-dialkyl-glycerol
52 tetraether, GDGT) and calditoglycerocaldarchaeol (or glycerol-dialkyl-nonitol tetraether,
53 GDNT), can include up to eight cyclopentane rings (Chong 2010; Chong et al. 2012).

54

55 To understand the importance of cyclopentane rings in the hydrophobic cores of
56 tetraether lipids, both *in vivo* and *in vitro* strategies have been adopted. Studies with
57 various strains have revealed that the number of cyclopentane rings increases as growth
58 temperature rises but decreases as medium pH becomes more acidic (Chong 2010; Boyd
59 et al 2011; Oger and Cario 2013; Jensen et al. 2015). Further insight into the importance
60 of the cyclopentane rings has come from biophysical analysis of liposomes based on

61 tetraether lipids. Differential scanning calorimetry and pressure perturbation calorimetry
62 studies revealed changes in the thermodynamic properties of such liposomes as a function
63 of whether or not the tetraether lipids contained cyclopentane rings (Chong et al. 2005).
64 Specifically, the presence of cyclopentane rings was proposed to make the membrane
65 tighter and more rigid. Molecular dynamics simulation studies support this concept
66 (Gabriel and Chong 2000). Others, however, failed to see reduced membrane leakiness as
67 the number of cyclopentane rings increased (Koyanagi et al. 2016). Cryo-transmission
68 electron microscopy and small angle X-ray scattering studies on synthetic tetraether lipids
69 containing cyclopentane rings have shown that the stereochemistry of cyclopentane rings
70 with the biphytanyl chains of tetraether lipids can affect the shape of multilamellar
71 vesicles composed of such lipids (Jacquemet et al. 2011; Jacquemet et al. 2012). At the
72 same time, the position of the cyclopentane ring apparently affects hydration properties,
73 lyotropic liquid crystalline behavior and membrane organization of vesicles comprising
74 tetraether lipids (Brard et al. 2004).

75

76 While advances into understanding the functions of the cyclopentane rings of GDGT- and
77 GDNT-based tetraether lipids have been made, virtually nothing is known of the steps
78 used to generate these moieties. In the present study, genes affecting the formation of
79 cyclopentane rings in a GDGT-based *Sulfolobus acidocaldarius* glycolipid were
80 identified for the first time.

81

82

83

84 MATERIALS AND METHODS

85 *Strains and growth*

86 *S. acidocaldarius* (MW001) (Wagner et al. 2012) and the same strain deleted of various
87 genes were grown at 75°C in Brock's medium (Brock et al. 1972), pH-adjusted to 3 using
88 sulphuric acid, supplemented with 0.1% (w/v) NZ-amine, 0.2% (w/v) dextrin and 10
89 µg/ml uracil, under constant shaking.

90

91 *Construction of deletion plasmids*

92 Marker-less deletion mutants of *Saci_0201*, *Saci_0275*, *Saci_0421*, *Saci_1101*,
93 *Saci_1201*, *Saci_1249* and *Saci_1706* were obtained in background strain *S.*
94 *acidocaldarius* MW001, as previously described (Wagner et al. 2009). To construct the
95 gene deletion plasmids pSVA1270, pSVA1231, pSVA1256, pSVA1228, pSVA1238,
96 pSVA1239, and pSVA1254, respectively containing the up- and downstream regions of
97 *Saci_0201*, *Sac_0275*, *Saci_421*, *Saci_1101*, *Saci_1201*, *Saci_1249*, and *Saci_1706*, 800–
98 1000 bp of the sequences found up- and downstream of each gene were PCR amplified.
99 At the 5'-ends of the upstream forward primer and the downstream reverse primer, *ApaI*
100 and *BamHI* restriction sites were introduced, respectively. The upstream reverse primers
101 and the downstream forward primers were designed to each incorporate 15 bp of the
102 reverse complement strand of the other primer, resulting in a 30 bp overlapping stretch.
103 All up- and downstream fragments were fused by overlapping PCR, using the 3'-ends of
104 the up- and downstream fragments as primers. The primers used to generate the deletion
105 strains are listed in Supplementary Table 1. The overlapping PCR fragments were
106 purified and digested with *ApaI* and *BamHI* and ligated in the pre-digested plasmid

107 pSVA407, containing *pyrEF* (Wagner et al. 2009). The deletion plasmids obtained (listed
108 in Supplementary Table 2) were transformed into *Escherichia coli* DH5 α and selected on
109 LB plates containing 50 mg/ml ampicillin. The accuracy of the plasmids was ascertained
110 by sequencing. To avoid restriction in *S. acidocaldarius*, the plasmids were methylated
111 by transformation in *E. coli* ER1821.

112

113 ***Transformation and selection of S. acidocaldarius deletion mutants***

114 Generation of competent cells was performed based on the protocol of Kurosawa and
115 Grogan as previously described (Kurosawa and Grogan, 2005). Methylated pSVA1270,
116 pSVA1231, pSVA1256, pSVA1228, pSVA1238, pSVA1239 or oSVA1254 (400–600 ng)
117 were added to a 50 μ l aliquot of competent MW001 cells and incubated for 5 min on ice,
118 before transformation in a 1 mm gap electroporation cuvette at 1250 V, 1000 Ω , 25 mF
119 using a Biorad Gene Pulser II (Biorad, Hercules CA). Directly after transformation 50 μ l
120 of a 2x concentrated recovery solution (1% sucrose, 20 mM β -alanine, 10 mM MgSO $_4$, 20
121 mM malate buffer, pH 4.5) were added to the sample, which was incubated at 75°C for 30
122 min under mild shaking conditions (150 rpm). Before plating, the sample was mixed with
123 100 μ l of heated 2x concentrated recovery solution and twice, 100 μ l were spread onto
124 gelrite plates containing Brock medium supplemented with 0.1% NZ-amine and 0.1%
125 dextrin. After incubation for 5–7 days at 75°C, large brownish colonies were used to
126 inoculate 50 ml of Brock medium containing 0.1% NZ-amine and 0.1% dextrin, which
127 were incubated for 3 days of 78°C. After confirming the presence of the integrated plasmid
128 by PCR, each culture was grown in Brock medium supplemented with 0.1% NZ-amine and
129 0.1% dextrin until an OD of 0.4. To confirm gene deletion, 40 μ l aliquots were spread onto

130 selection plates supplemented with 0.1% NZ-amine, 0.1% dextrin and 10 mg/ml uracil, and
131 incubated for 5–7 days at 78°C. Newly formed colonies were streaked out on new selection
132 plates to ensure that they were formed from single colonies, before each was screened for
133 the absence or presence of the deleted genes by PCR.

134

135 *S. acidocaldarius* lipid extraction

136 *S. acidocaldarius* lipid extraction was performed essentially as described previously
137 (Murae et al. 2001). Briefly, a solution (2 ml) of CHCl₃:MetOH (2:1, v/v) was added to a
138 *S. acidocaldarius* cell pellet (~ 800 µl). The pellets were manually homogenized with a
139 glass homogenizer and sonicated in a Elmasonic bath sonicator for 30 minutes at room
140 temperature. The homogenate was centrifuged for 10 min at 10,000 g at 4°C. The
141 supernatant was removed and transferred into a fresh 15 ml Falcon tube. A solution (2
142 ml) of CHCl₃:MetOH (1:2, v/v) was added to the pellet, which was homogenized in a
143 glass homogenizer, sonicated for 30 minutes and centrifuged for 10 min at 10,000 g at
144 4°C. The supernatant was removed and transferred to the tube containing the previous
145 supernatant. The second set of homogenization, sonication, centrifugation and removal of
146 supernatant steps was repeated two more times. The combined supernatants were then
147 filtered through a 0.22 µm syringe PVDF filter (Merck Millipore) and evaporated to
148 dryness under a stream of N₂.

149

150 *High performance liquid chromatography-electrospray ionization mass spectrometry*

151 *(HPLC-ESI MS) analysis of the S. acidocaldarius lipid extract*

152 Normal phase HPLC-ESI MS of the *S. acidocaldarius* lipid extract was performed using
153 an Agilent 1200 Quaternary LC system coupled to a high resolution TripleTOF5600 mass
154 spectrometer (Sciex, Framingham, MA). Chromatographic separation was performed on
155 an Ascentis Silica HPLC column, 5 μm , 25 cm x 2.1 mm (Sigma-Aldrich, St. Louis,
156 MO). Elution was achieved with mobile phase A, consisting of
157 chloroform/methanol/aqueous ammonium hydroxide (800:195:5, v/v/v), mobile phase B,
158 consisting of chloroform/methanol/water/aqueous ammonium hydroxide (600:340:50:5,
159 v/v/v/v) and mobile phase C, consisting of chloroform/methanol/water/aqueous
160 ammonium hydroxide (450:450:95:5, v/v/v/v), over a 40 min-long run, performed as
161 follows: 100% mobile phase A was held isocratically for 2 min and then linearly
162 increased to 100% mobile phase B over 14 min and held at 100% B for 11 min. The
163 mobile phase composition was then changed to 100% mobile phase C over 3 min and
164 held at 100% C for 3 min, and finally returned to 100% A over 0.5 min and held at 100%
165 A for 5 min. The LC eluent (with a total flow rate of 300 $\mu\text{l}/\text{min}$) was introduced into the
166 ESI source of the high resolution TF5600 mass spectrometer, with MS settings as
167 follows: Ion spray voltage (IS) = -4500 V, Curtain gas (CUR) = 20 psi, Ion source gas 1
168 (GS1) = 20 psi, De-clustering potential (DP) = -55 V, and Focusing Potential (FP) = -150
169 V. Samples were analyzed in negative-ion mode, with the full-scan spectra being
170 collected in the m/z 300-2000 range. Nitrogen was used as the collision gas (collision
171 energy = 40 eV) for tandem mass spectrometry (MS/MS) experiments. Data acquisition
172 and analysis were performed using Analyst TF1.5 software (Sciex, Framingham, MA).

173 **RESULTS**

174 *Deletion of Saci_0421 and Saci_1201 leads to decreased numbers of cyclopentane*
175 *rings*

176 As part of ongoing efforts aimed at defining novel components of the pathway for protein
177 N-glycosylation in *S. acidocaldarius*, a number of genes encoding products suspected of
178 contributing to this post-translational modification (*Saci_0201*, *Saci_0275*, *Saci_0421*,
179 *Saci_1101*, *Saci_1201*, *Saci_1249* and *Saci_1706*) were deleted. LC-ESI MS analysis of
180 FlaB and SlaA, two reporter glycoproteins previously shown to be modified by an N-
181 linked hexasaccharide (Peyfoon et al. 2010; Guan et al. 2016), as well as the dolichol
182 pyrophosphate carrier upon which this glycan is assembled (Guan et al. 2016), revealed
183 patterns of glycosylation in the deletion strains identical to what was seen for these same
184 molecules isolated from the parent strain (not shown). Given that distinct genes
185 contribute to protein glycosylation and lipid glycosylation in the halophilic archaea
186 *Haloferax volcanii* (Naparstek, Vinogradov and Eichler 2010), efforts next focused on
187 assessing whether the absence of *Saci_0201*, *Saci_0275*, *Saci_0421*, *Saci_1101*,
188 *Saci_1201*, *Saci_1249* or *Saci_1706* had any effect on *S. acidocaldarius* glycolipids.
189

190 The *S. acidocaldarius* membrane contains tetraether glycolipids based on GDGT
191 presenting phospho-*myo*-inositol attached to glycerol at one end of the molecule and β -D-
192 galactosyl-D-glucose attached to the glycerol at the other end (De Rosa, Gambacorta and
193 Nicolaus 1983) (Fig 1A). Accordingly, when a total *S. acidocaldarius* lipid extract from
194 the MW001 parent strain was assessed by LC-ESI MS, a species with a [M-H]⁻
195 monoisotopic ion peak at m/z 1858.425, corresponding to this glycolipid (calculated mass

196 1858.37 Da; error 30 ppm), was detected (Fig 1B). Analysis of the product spectrum
197 obtained upon MS/MS analysis of the doubly charged $[M-H+Cl]^{2-}$ ion at m/z 946.784
198 showed peaks consistent with this species (Fig 1C). Furthermore, the monoisotopic ion
199 peaks at m/z 1696.32 and 1534.27 are consistent with the $[M-H]^-$ ions of precursors or
200 derivatives of the trisaccharide-containing glycolipid modified by either two or one
201 hexoses, respectively (calculated masses 1696.37 and 1534.37Da, with the m/z 1696.32
202 species containing two hexoses, and the m/z 1534.27 species containing only one hexose),
203 were also observed (not shown). The masses of the different variants of the glycolipid
204 detected are consistent with the presence of four cyclopentane rings, with two assumed to
205 be in each phytanyl chain.

206

207 When lipid extracts prepared from *S. acidocaldarius* strains deleted of *Saci_0275*,
208 *Saci_1101* or *Saci_1249* were similarly assessed, $[M-H]^-$ monoisotopic ion peaks at m/z
209 1858.378, 1858.376 and 1858.373, respectively, were observed (Fig 1D). Similar peaks
210 were also detected in the lipid extracts of strains lacking *Saci_0201* or *Saci_1706* (not
211 shown). In addition, precursors or derivatives of the trisaccharide-containing glycolipid
212 modified by either two or one hexoses were also seen in these deletion strains (not
213 shown). It would thus appear that these mutants contain the same trisaccharide-bearing
214 glycolipid as found in the parent strain.

215

216 At the same time, closer examination of the LC-ESI MS profiles obtained for two of the
217 mutant strains, $\Delta Saci_0421$ and $\Delta Saci_1201$, revealed additional peaks not seen in the
218 profiles of the other strains considered above (Fig 2A; compare with Fig 1B, D). These

219 peaks, showing incremental 2 Da increases, represent species possessing fewer degrees of
220 unsaturation, and are consistent with variants of the trisaccharide-charged glycolipid
221 containing fewer than four cyclopentane rings, as supported by isotopic distribution
222 simulations (Fig 2B). Simulation of the isotopic distribution of the glycolipid containing
223 four, two and zero cyclopentane rings shows that the expected profiles resemble what
224 was observed in the $\Delta Saci_0421$ and $\Delta Saci_1201$ profiles (compare Fig 2A and Fig 2B).
225 It is unlikely that these additional peaks reflect an expansion of the isotopic distribution
226 of the $[M-H]^-$ monoisotopic ion peak associated with the trisaccharide-charged
227 glycolipid observed at m/z 1858.37 due to a higher amount of this species in the
228 $\Delta Saci_0421$ and $\Delta Saci_1201$ lipid extracts as the intensity of this peak from these species
229 was considerably lower than that of the same peak from the parent strain and the
230 $\Delta Saci_0275$, $\Delta Saci_1101$ and $\Delta Saci_1249$ mutants (compare peak intensities in Fig 1B
231 and 1D with those in Fig 2A). Moreover, the major peak in the profile from the
232 $\Delta Saci_1201$ sample was not observed at m/z 1858.37 but rather at m/z 1862.39.
233 Moreover, additional peaks in the LC-ESI MS profiles of the di- and monosaccharide-
234 charged precursors/derivatives of the complete trisaccharide-charged glycolipid, again
235 representing species presenting fewer degrees of unsaturation, were also observed in the
236 $\Delta Saci_0421$ and $\Delta Saci_1201$ mutant strains but not in the profiles of the other strains
237 considered (not shown).

238

239 The possibility that the extra peaks seen in the LC-ESI MS profiles of the $\Delta Saci_0421$
240 and $\Delta Saci_1201$ strains represent variants of the trisaccharide-charged glycolipid (and its
241 di- and monosaccharide-charged precursors/derivatives) containing fewer than four

242 cyclopentane rings was more directly considered. Specifically, the $[M-H+Cl]^{2-}$ ion peak
243 observed at m/z 950.70 in the total lipid extract from the $\Delta Saci_0421$ species was
244 subjected to MS/MS analysis. The product spectrum of this species was consistent with
245 chlorine adduct of the trihexose-charged glycolipid lacking cyclopentane rings (Fig 2C).
246 Therefore, it appears that *Saci_0421* (and *Saci_1201*) contributes to the appearance of
247 cyclopentane rings in the polyisoprene chains of the GDGT moiety of the *S.*
248 *acidocaldarius* glycolipid considered here, and possibly in other tetraether lipids in this
249 species.

250

251 Finally, given the reported increase in cyclopentane ring content of *S. acidocaldarius*
252 tetraether lipids as the growth temperature rises (De Rosa et al. 1980), mutants in which
253 cyclopentane ring content is compromised would be expected to grow less well at
254 elevated temperatures than would the parent strain. No differences in the growth rates of
255 the $\Delta Saci_0421$ and $\Delta Saci_1201$ mutants and the parent strain were observed when the
256 cells were grown at either standard (75°C) or elevated (80°C) growth temperatures.

257

258 ***Homologues of Saci_0421 and Saci_1201 are found in other (hyper)thermophiles***

259 To determine whether genes in the vicinity of *Saci_0421* (currently annotated as
260 encoding a dolichyl-phosphate-mannose-protein mannosyltransferase termed Ag11, given
261 its putative role in N-glycosylation (Meyer et al. 2011)) and/or *Saci_1201* (currently
262 currently annotated as encoding a glycogen synthase) might also encode proteins
263 putatively involved in cyclopentane ring, GDGT or tetraether lipid assembly, the putative
264 products of the twelve open reading frames lying upstream and downstream of each gene

265 were considered (Supplementary Table 3). *Saci_0422* (*agl2*), *Saci_0423* (*agl3*) and
266 *Saci_0424* (*agl4*) are predicted to encode proteins that participate in N-glycosylation in *S.*
267 *acidocaldarius*, with experimental proof for the role of *Saci_0423* (*Agl3*) as a
268 sulfoquinovose synthase having been provided (Meyer et al. 2011). *Saci_0422* (*agl2*) and
269 *Saci_0424* (*agl4*) are predicted to encode a dTDP-glucose pyrophosphorylase and a
270 glucokinase, respectively (Meyer et al. 2011). Other annotated genes in this region and in
271 the region surrounding *Saci_1201* are currently predicted to encode proteins serving
272 various roles, and many are listed as encoding conserved or hypothetical proteins. As
273 such, it would appear that neither *Saci_0421* nor *Saci_1201* belong to an operon or gene
274 cluster involved in tetraether lipid biogenesis.

275

276 Finally, efforts were aimed at determining whether homologues of *Saci_0421* and/or
277 *Saci_1201* are found in other Archaea where cyclopentane-containing tetraether lipids are
278 found. BLAST searches using *Saci_0421* as query detected the presence of homologues
279 in various species (Supplementary Table 4). Although all are (hyper)thermophiles, the
280 presence of tetraether lipids containing cyclopentane rings has been demonstrated in only
281 a few of these species other than *Sulfolobus acidocaldarius* (De Rosa et al. 1980), such as
282 *Thermoproteus tenax* (Thurl and Schafer 1988), *Sulfolobus solfataricus* (De Rosa,
283 Gambacorta and Gliozzi 1986) and *Pyrococcus horikoshii* (Sugai et al. 2000). At the
284 same time, no *Saci_0421* homologues were detected in other species, such as
285 *Thermoplasma acidophilum* or *Archaeoglobus fulgidus*, where cyclopentane-containing
286 tetraether lipids have been described (Shimida et al. 2002; Lai, Springstead and
287 Monbouquette 2008). When *Saci_1201* served as query in a BLAST search, homologues

288 were also detected in a variety of species (Supplementary Table 5). Again, those species
289 containing the homologous sequences are all (hyper)thermophiles, although this list was
290 not identical to that of species containing Saci_0421 homologues.

291 **DISCUSSION**

292 As the numbers of archaeal genome sequences and strains for which genetic tools are
293 available grow, a clearer picture of archaeal biochemistry and those aspects unique to this
294 life form is emerging. Still, much remains to be clarified. In the case of the tetraether
295 lipids that comprise the membranes of (hyper)thermophilic archaea, many biosynthetic
296 steps either remain as predictions, such the presumed coupling of two archaeol lipids to
297 generate GDGT (Koga and Morii 2007; Villanueva et al. 2014), or completely undefined,
298 such as the steps leading to the appearance of cyclopentane rings in each of the phytanyl
299 chains of such lipids. In the present report, the deletion of specific genes was shown for
300 the first time to affect cyclopentane ring formation in a *S. acidocaldarius* glycolipid.
301 Specifically, the deletion of *Saci_0421* and *Saci_1201*, currently annotated as encoding a
302 dolichyl-phosphate-mannose-protein mannosyltransferase and a glycogen synthase,
303 respectively, led to the formation of a GDGT moiety within a trihexose-bearing
304 glycolipid with reduced numbers or even lacking cyclopentane rings. In the presence of
305 these genes, both in the parent strain and in a series of other *S. acidocaldarius* deletion
306 strains, the GDGT moiety largely contained four cyclopentane rings under the growth
307 conditions employed here.

308

309 It was previously reported that the number of cyclopentane rings in GDGT is affected not
310 only by growth temperature and pH but also by stirring of the cell cultures when growing
311 and by the method used for lipid extraction (Uda et al. 2001). Since the various *S.*
312 *acidocaldarius* strains considered here were all similarly grown and processed, it is
313 unlikely that the observed effects of *Saci_0421* and *Saci_1201* deletion on glycolipid

314 cyclopentane ring content reflect growth- or preparation-related effects. Instead, it would
315 seem that the observed effects of deleting these genes on cyclopentane content are
316 biologically relevant. Based on what is known of tetraether lipid biosynthesis (Koga and
317 Morii 2007; Villanueva et al. 2014), two scenarios leading to the appearance of
318 cyclopentane rings within a GDGT (or GDNT) hydrophobic core can be envisaged. In the
319 first, internal cyclization of saturated phytanyl chains would occur. Alternatively,
320 cyclopentane rings would be present in the prenyl groups being added to the growing
321 chain. However, reports of the number of cyclopentane rings changing as a function of
322 growth temperature and growth phase (Chong 2010; Oger and Cario 2013; Jensen et al.
323 2015 and references therein) are difficult to reconcile with this second scenario, unless
324 substantial lipid turnover occurs. It should be noted that no change in cyclopentane ring
325 content was seen when the growth temperature was raised from 75 to 80°C in the present
326 study; this could be related to the particular growth conditions employed. It is even less
327 clear how enzymes thought to be involved in sugar/polysaccharide processing and/or
328 assembly, such as Saci_0421 or Saci_1201 (Cardona et al. 2001), could contribute to the
329 appearance of cyclopentane rings. While it is possible that they somehow contribute to
330 the cyclization process presumably involved in cyclopentane ring biogenesis, one can
331 also imagine that these proteins instead modify some other aspect of the membrane, with
332 the observed drop in ring numbers being an indirect effect resulting from the loss of the
333 predicted functions of Saci_0421 or Saci_1201.

334

335 The identification of tetraether lipids represents yet another example of how the study of
336 Archaea has expanded our appreciation of the diverse solutions Nature provides to a

337 given challenge. Indeed, different versions of tetraether lipids isolated from a range of
338 archaeal species that thrive in a variety of environments and that present distinct chemical
339 modifications affecting the functions of such lipids, have been described (Damsté et al.
340 2002; Knappy et al. 2011). Understanding of the biosynthetic pathways involved in
341 generating such variability is, however, lacking. The present study represents a step
342 towards addressing this gap.

343 **FUNDING**

344 This work was supported by the German-Israeli Foundation for Scientific Research and
345 Development (grant I-1290- 416.13/2015) to S.V.A. and J.E. The mass spectrometry
346 facility in the Department of Biochemistry of the Duke University Medical Center and
347 Z.G. were supported by the National Institutes of Health (grants GM-069338 and
348 EY023666). B.M. received support from a European Research Council starting grant
349 (grant 311523, ARCHAELLUM).

350

351 **CONFLICTS OF INTEREST**

352 The authors declare no conflicts of interest.

353 **REFERENCES**

- 354 Boyd ES, Pearson A, Pi Y et al. Temperature and pH controls on glycerol dibiphytanyl
355 glycerol tetraether lipid composition in the hyperthermophilic crenarchaeon *Acidilobus*
356 *sulfurireducens*. *Extremophiles* 2011;15:59-65.
357
- 358 Brard M, Richler M, Benvegu T et al. Synthesis and supramolecular assemblies of
359 bipolar archaeal glycolipid analogues containing a cis-1,3-disubstituted cyclopentane
360 ring. *J Am Chem Soc* 2004;126:10003-12.
361
- 362 Brock TD, Brock KM, Belly RT et al. *Sulfolobus*: a new genus of sulfur-oxidizing
363 bacteria living at low pH and high temperature. *Arch Mikrobiol* 1972;84:54-68.
364
- 365 Cardona S, Remonsellez F, Guiliani N, et al. The glycogen-bound
366 polyphosphate kinase from *Sulfolobus acidocaldarius* is actually a glycogen
367 synthase. *Appl Environ Microbiol* 2001;67:4773-80.
368
- 369 Chong PL. Archaeobacterial bipolar tetraether lipids: Physico-chemical and membrane
370 properties. *Chem Phys Lipids* 2010;163:253-65.
371
- 372 Chong PL, Ravindra R, Khurana M et al. Pressure perturbation and differential scanning
373 calorimetric studies of bipolar tetraether liposomes derived from the thermoacidophilic
374 archaeon *Sulfolobus acidocaldarius*. *Biophys J* 2005;89:1841-9.
375
- 376 Chong PL, Ayesa U, Daswani VP et al. On physical properties of tetraether lipid
377 membranes: effects of cyclopentane rings. *Archaea* 2012;2012:138439.
378
- 379 Damsté JS, Schouten S, Hopmans EC et al. Crenarchaeol: the characteristic core glycerol
380 dibiphytanyl glycerol tetraether membrane lipid of cosmopolitan pelagic crenarchaeota. *J*
381 *Lipid Res* 2002;43:1641-51.
382
- 383 De Rosa M, Esposito E, Gambacorta A et al. Effects of temperature on ether lipid
384 composition of *Caldariella acidophila*. *Phytochemistry* 1980;19:827-31.
385
- 386 De Rosa M, Gambacorta A, Nicolaus B. A new type of cell membrane in
387 thermophilic archaeobacteria based on bipolar ether lipids. *J Membr Sci* 1983;16:287-94.
388
- 389 De Rosa M, Gambacorta A, Gliozzi A. Structure, biosynthesis, and physicochemical
390 properties of archaeobacterial lipids. *Microbiol Rev* 1986;50:70-80.
391
- 392 Gabriel JL, Chong PL. Molecular modeling of archaeobacterial bipolar tetraether lipid
393 membranes. *Chem Phys Lipids* 2000;105:193-200.
394
- 395 Guan Z, Delago A, Nussbaum P et al. N-glycosylation in the thermoacidophilic archaeon
396 *Sulfolobus acidocaldarius* involves a short dolichol pyrophosphate carrier. *FEBS Lett*
397 2016;590:3168-78.

398
399 Jacquemet A, Lemiegre L, Lambert O et al. How the stereochemistry of a central
400 cyclopentyl ring influences the self-assembling properties of archaeal lipid
401 analogues: synthesis and cryoTEM observations. *J Org Chem.* 2011;76:9738-47.
402
403 Jacquemet A, Meriadec C, Lemiegre L et al. Stereochemical effect revealed in self-
404 assemblies based on archaeal lipid analogues bearing a central five-membered
405 carbocycle: a SAXS study. *Langmuir* 2012;28:7591-7.
406
407 Jensen SM, Neesgaard VL, Skjoldbjerg SL et al. The effects of temperature and growth
408 phase on the lipidomes of *Sulfolobus islandicus* and *Sulfolobus tokodaii*. *Life*
409 2015;5:1539-66.
410
411 Knappy CS, Nunn CE, Morgan HW et al. The major lipid cores of the archaeon
412 *Ignisphaera aggregans*: implications for the phylogeny and biosynthesis of
413 glycerol monoalkyl glycerol tetraether isoprenoid lipids. *Extremophiles* 2011;15:517-28.
414
415 Koga Y, Morii H. Biosynthesis of ether-type polar lipids in archaea and evolutionary
416 considerations. *Microbiol Mol Biol Rev* 2007;71:97-120.
417
418 Koyanagi T, Leriche G, Onofrei D et al. Cyclohexane rings reduce membrane
419 permeability to small ions in Archaea-inspired tetraether lipids. *Angew Chem Int Ed Engl*
420 2016;55:1890-3.
421
422 Kurosawa N, Grogan DW. Homologous recombination of exogenous DNA with the
423 *Sulfolobus acidocaldarius* genome: properties and uses. *FEMS Microbiol Lett* 2005
424 ;253:141-9.
425
426 Lai D, Springstead JR, Monbouquette HG.. Effect of growth temperature on
427 ether lipid biochemistry in *Archaeoglobus fulgidus*. *Extremophiles* 2008;12:271-8.
428
429 Meyer BH, Zolghadr B, Peyfoon E et al. Sulfoquinovose synthase – an important enzyme
430 in the N-glycosylation pathway of *Sulfolobus acidocaldarius*. *Mo. Microbiol*
431 2011;82:1150-63.
432
433 Murae T, Muraoka R, Kitajima F. Examination of intact ether lipid components of
434 thermoacidophile *Sulfolobus sp.* by ESI/TOF mass spectrometry. *J Mass Spectrom Soc*
435 *Jpn* 2001;49:195-200.
436
437 Naparstek S, Vinogradov E, Eichler J. Different glycosyltransferases are involved in lipid
438 glycosylation and protein N-glycosylation in the halophilic archaeon *Haloferax volcanii*.
439 *Arch Microbiol* 2010;192:581-4.
440
441 Oger PM, Cario A. Adaptation of the membrane in Archaea. *Biophys Chem* 2013;183:42-
442 56.
443

444 Peyfoon E, Meyer B, Hitchen PG, et al. The S-layer glycoprotein of the crenarchaeote
445 *Sulfolobus acidocaldarius* is glycosylated at multiple sites with the chitobiose-linked N-
446 glycans. *Archaea* 2010;2010:754101.
447
448 Shimada H, Shida Y, Nemoto N et al. Complete polar lipid composition of
449 *Thermoplasma acidophilum* HO-62 determined by high-performance liquid
450 chromatography with evaporative light-scattering detection. *J Bacteriol* 2002;184:556-63.
451
452 Sugai A, Masuchi Y, Uda I et al. Core lipids of hyperthermophilic archaeon. *Pyrococcus*
453 *horikoshii* OT3. *J Jpn Oil Chem Soc* 2000;49:695–700.
454
455 Thurl S, Schäfer W. Lipids from the sulphur-dependent archaeobacterium *Thermoproteus*
456 *tenax*. *Biochim Biophys Acta* 1988;961:253–261.
457
458 Villanueva L, Damsté JS, Schouten S. A re-evaluation of the archaeal membrane lipid
459 biosynthetic pathway. *Nat Rev Microbiol* 2014;12:438-48.
460
461 Wagner M, Berkner S, Ajon M, Driessen AJ, Lipps G, Albers SV. Expanding and
462 understanding the genetic toolbox of the hyperthermophilic genus *Sulfolobus*.
463 *Biochem Soc Trans* 2009;37:97-101.
464
465 Wagner M, van Wolferen M, Wagner A, et al. Versatile genetic toolbox for the
466 crenarchaeote *Sulfolobus acidocaldarius*. *Front Microbiol* 2012;3:214.
467

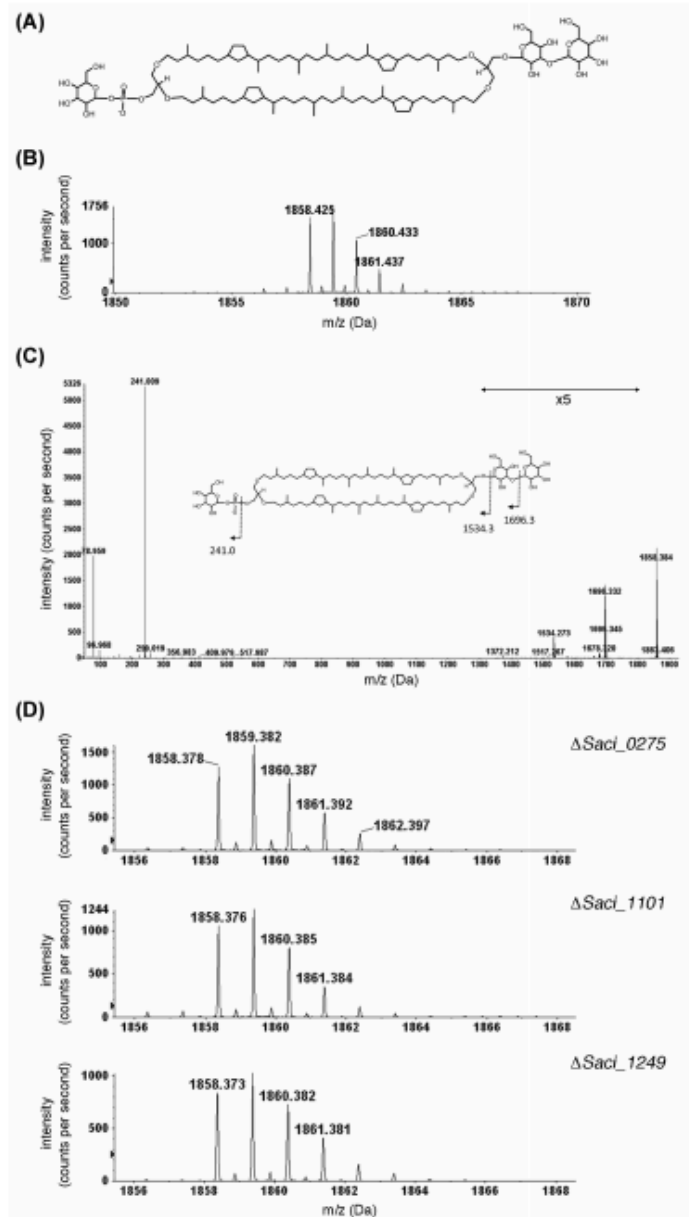


Figure 1. Detection of a *S. acidocaldarius* glycolipid containing four cyclopentane rings. (A) Schematic depiction of a glycolipid based on GDGT and modified by a phosphate group and three hexoses and including four cyclopentane rings evenly distributed between the two phytanyl chains. (B) *Sulfolobus acidocaldarius* cells present a $[M-H]^-$ monoisotopic ion peak at m/z 1858.425 corresponding to the glycolipid (calculated mass 1858.37 Da). (C) MS/MS spectrum of the $[M-H + Cl]^-$ ion at m/z 946.784 (Cl^- chloride ion). The inset schematically represents the fragmentation schema. The arrows indicating $\times 5$ reflect magnification of the ion peaks in the corresponding region of the m/z values on the graph. (D) *Sulfolobus acidocaldarius* Δ SacI_0275, Δ SacI_1101 and Δ SacI_1249 present a $[M-H]^-$ monoisotopic ion peak at m/z 1858.37 corresponding to the glycolipid depicted in panel A.

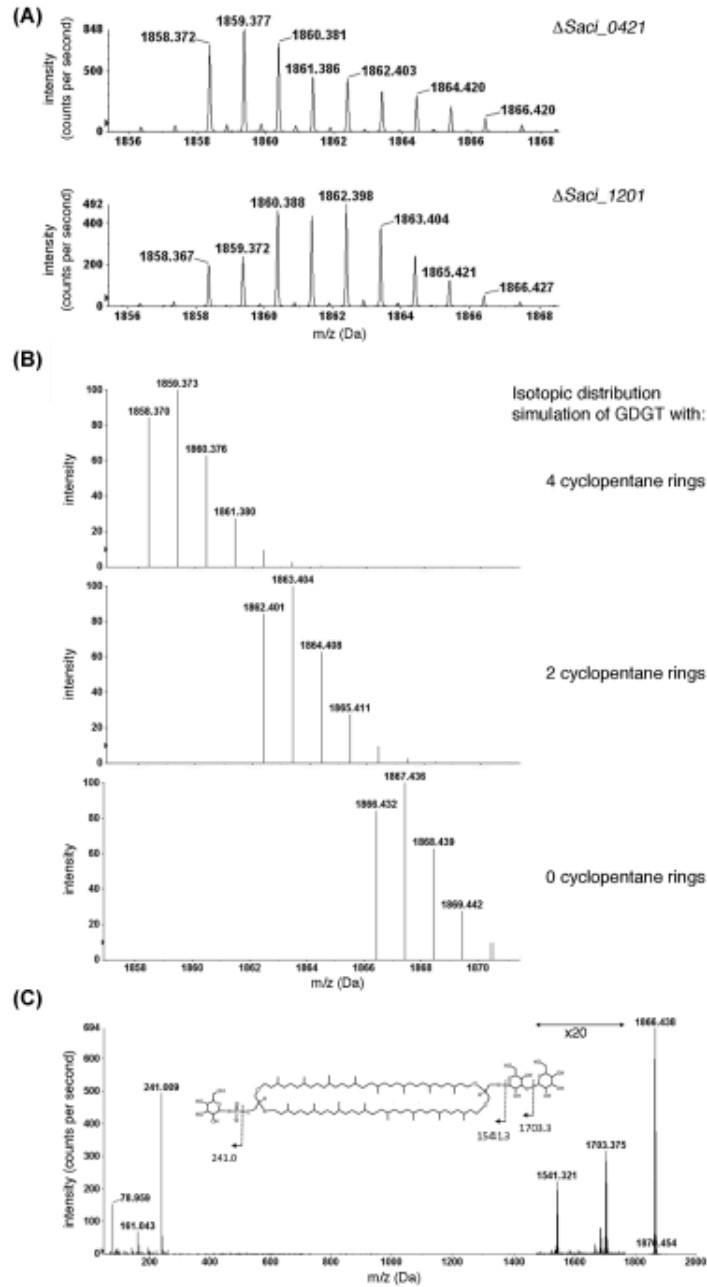


Figure 2. The same glycolipid in *S. acidocaldarius* Δ SacI₀₄₂₁ and Δ SacI₁₂₀₁ cells contains 0–4 cyclopentane rings. (A) *Sulfolobus acidocaldarius* Δ SacI₀₄₂₁ and Δ SacI₁₂₀₁ present a $[M-H]^-$ monoisotopic ion profile containing additional peaks not seen in parent strain, and Δ SacI₀₂₇₅, Δ SacI₁₁₀₁ or Δ SacI₁₂₄₉ cells. (B) Simulation of the isotopic distribution of the glycolipid containing four, two and zero cyclopentane rings, as indicated. (C) MS/MS spectrum of the $[M-H + Cl]^-$ ion at m/z 950.70. The inset schematically represents the fragmentation scheme. The arrows indicating $\times 20$ reflect magnification of the ion peaks in the corresponding region of the m/z values on the x-axis.